Published in final edited form as:
Circ Res. 2008 September 26; 103(7): 743–750. doi:10.1161/CIRCRESAHA.108.172858.

Tbx3 is required for outflow tract development

Karim Mesbah[1], **Zachary Harrelson**[2,+], **Magali Théveniau-Ruissy**[1], **Virginia E. Papaioannou**[2], and **Robert G. Kelly**[1,*]

[1] Developmental Biology Institute of Marseilles-Luminy, Inserm Avenir group, UMR 6216 CNRS-Université de la Méditerranée, Campus de Luminy, Case 907, 13288 Marseille Cedex 9, France

[2] College of Physicians and Surgeons of Columbia University, 701 W 168th St., New York, NY 10032, USA

Abstract

Conotruncal and ventricular septal congenital heart anomalies result from defects in formation and division of the embryonic outflow tract. Cardiac remodeling during outflow tract and ventricular septation converts the tubular embryonic heart into a parallel circulatory system with an independent left ventricular outlet and right ventricular inlet. *Tbx3* encodes a T-box containing transcription factor expressed in the developing conduction system of the heart. Mutations in *TBX3* cause Ulnar-Mammary syndrome. Here we show that mice lacking *Tbx3* develop severe outflow tract defects, including connection of both the aorta and pulmonary trunk with the right ventricle, in addition to aortic arch artery anomalies and abnormal communication between the right atrium and left ventricle. Alignment defects are preceded by a delay in caudal displacement of the arterial pole during aortic arch artery formation. Embryonic anterior/posterior patterning and cardiac chamber development are unaffected in *Tbx3* mutant embryos. However, the contribution of second heart field derived progenitor cells to the arterial pole of the heart is impaired. *Tbx3* is expressed in pharyngeal epithelia and neural crest cells in the pharyngeal region suggesting an indirect role in second heart field deployment. Loss of Tbx3 affects multiple signaling pathways regulating second heart field proliferation and outflow tract morphogenesis, including fibroblast growth factor signaling, leading to a failure of normal heart tube extension and consequent atrioventricular and ventriculoarterial alignment defects.

Keywords

Tbx3; outflow tract; congenital heart defect; neural crest

Introduction

Morphogenesis of the arterial pole of the heart involves formation and subsequent division of the myocardial outflow tract (OFT) to generate the ascending aorta and pulmonary trunk connected to the left and right ventricles, respectively [1]. This complex process requires interactions between myocardial, endocardial and neural crest-derived (NC) cells. Defects in OFT morphogenesis in man and mouse models result in congenital heart anomalies including abnormal ventriculoarterial alignment such as double outlet right ventricle and

[*]Correspondence to: Robert G. Kelly, IBDML, Campus de Luminy Case 907, 13288 Marseille Cedex 9, France, Tel: 33-491269732, Fax: 33-491269726, kelly@ibdml.univ-mrs.fr.
[+]Current address: Skaggs School of Pharmacy, University of California, San Diego, 9500 Gilman Drive, La Jolla, California, USA

Disclosures
None

overriding aorta, associated with ventricular septal defects. The myocardial wall of the OFT is derived from progenitor cells of the second heart field (SHF), a population of pharyngeal mesodermal cells expressing the transcription factors Isl1 and Tbx1[2]. Contribution of SHF derived myocardium to the heart tube is essential for normal elongation of the heart tube and subsequent ventriculoarterial alignment [3]. Division of the OFT occurs concomitantly with ventricular septation and is driven by cardiac NC cells [4]. Prior to their entry into the OFT, NC cells are required in the pharyngeal region for normal addition of SHF cells to the distal heart tube [3,5].

T-box containing transcription factors control multiple aspects of embryonic development including morphogenesis and patterning of the heart; haploinsufficiency or mutation in a number of *Tbx* genes in man and mouse result in congenital heart defects (reviewed in [6,7]). *Tbx2* and *Tbx3* are closely related paralogs of the T-box family with many areas of overlapping gene expression during development [8]. They act as transcriptional repressors and have at least some target genes in common, including regulators of proliferation and senescence [6]. *Tbx2* null embryos display cardiac abnormalities, including atrioventricular canal (AVC) anomalies and defects in OFT alignment [9]. *Tbx3* null embryos die over a range of several days during midgestation with severe but variable yolk sac abnormalities in addition to hindlimb defects and mammary gland aplasia [10]. *TBX3* mutations underlie Ulnar-Mammary syndrome in man [11]. The cause of lethality in *Tbx3* mutant embryos is uncertain, although cardiac abnormalities could be a contributing factor. *Tbx3* is expressed in the AVC and the sinoatrial and central components of the cardiac conduction system[12]. *Tbx2* represses the transcriptional program of ventricular and atrial myocardium in the AVC, and gain and loss of function experiments have demonstrated that *Tbx3* is required for sinoatrial node identity [9,13–16]. In addition, a recent report has described abnormalities in cardiac looping in mice carrying a novel *Tbx3* mutation ($Tbx3^{neo/neo}$)[17].

Here we show that *Tbx3* is required for arterial pole morphogenesis. In $Tbx3^{-/-}$ embryos elongation of the arterial pole of the heart is perturbed resulting in double outlet right ventricle, where both the aorta and pulmonary trunk are aligned with the right ventricle. *Tbx3* is expressed in pharyngeal epithelia and NC cells in the pharyngeal region and loss of *Tbx3* function is associated with elevated proliferation and defective deployment of SHF cells. Our data suggest that *Tbx3* regulates multiple signaling pathways required for normal SHF development and OFT elongation.

Materials and Methods

Mice

The null alleles $Tbx3^{tm1Pa}$ and $Tbx2^{tm1Pa}$ (hereafter referred to as $Tbx2^{-}$ and $Tbx3^{-}$) were maintained on a mixed genetic background [9,10]. Genotyping details are provided in the online data supplement. $Connexin40^{eGFP}$ and *Mlc1v-nlacZ-24* transgenic mice were genotyped as described [18,19]. Mouse care and procedures were in accordance with institutional and US and French national guidelines.

Histology and immunochemistry

Details of procedures are provided in the online data supplement. Primary antibody concentrations were: Tbx3 (1/200, Santa Cruz Biotechnology), β-galactosidase (1/300, Cappel), MF20 (1/50, DSHB), Islet-1 (clone 40.2D6: 1/100, DSHB), rat anti-BrdU (1/100, Immunologics), AP-2α (clone 3B5; 1/50, DSHB), phospho-ERK (1/100, Cell Signaling).

In situ hybridization

Whole mount in situ hybridization was performed as previously described [19]. For each experiment a minimum of 3 embryos of each genotype was scored. Details of riboprobes used are provided in the online data supplement.

Cell proliferation analysis

Cell proliferation was evaluated by bromodeoxyuridine (BrdU) incorporation. Pregnant females were injected intraperitoneally on E9 with 10μM of BrdU (Sigma) per 100g of body weight 1.5hrs prior to embryo harvest. Embryos were sectioned, followed by immunochemical detection of BrdU-incorporated cells.

Quantitative RT-PCR

Details of procedures and primer sequences are provided in the online data supplement.

Results

Outflow tract and atrioventricular alignment defects in *Tbx3*$^{-/-}$ embryos

Tbx3$^{-/-}$ embryos surviving to E12.5 display a defect in leftward positioning and ventricular alignment of the ascending aorta (Figure 1, Table I). 12/12 embryos scored at E12.5 and E13.5 displayed double outlet right ventricle (DORV) such that the ascending aorta was aligned with the right rather than left ventricle. Ventricular septation, normally complete by E13.5, was incomplete in *Tbx3*$^{-/-}$ hearts at E13.5 (6/6). Two types of DORV were observed in *Tbx3*$^{-/-}$ embryos. In the first type, the ascending aorta is dextraposed such that the aorta and pulmonary trunk emerge from the right ventricle in a side-by-side configuration (5/12 embryos; Figure 1B). In the second type the aorta is positioned ventrally, a configuration resembling transposition of the great arteries (7/12 embryos; Figure 1C, G, J); histological analysis revealed that the pulmonary trunk is contiguous with cushion mesenchyme in the inner curvature of the OFT (Figure 1H, K). In addition to defects in alignment of the ascending aorta, aortic arch artery anomalies were observed in *Tbx3*$^{-/-}$ embryos, including persistence of the right 4th (9/12 embryos; Table 1 and Figure 1J) and right 6th (5/12; Table 1 and Figure 1K) arch arteries. Atrioventricular alignment defects were also observed in *Tbx3*$^{-/-}$ hearts; the right atrium frequently connected with the left rather than right ventricle, a configuration termed double inlet left ventricle (9/12 hearts; Figure 1I, L). *Tbx3*$^{-/-}$ hearts therefore display defective ventriculoarterial and atrioventricular alignment such that both great arteries emerge from the right ventricle and both atria connect with the left ventricle.

Tbx3 is required for complete cardiac looping

Cardiac looping is a prerequisite for correct alignment of the future cardiac chambers. Looping is a multistep process involving ventral then rightward looping of the elongating heart tube, followed by displacement of the inflow region of the heart dorsal to the ventricular segment, a process termed convergence [20]. We observed a high incidence of *Tbx3*$^{-/-}$ embryos in which convergence was delayed or defective compared to somite matched *Tbx3*$^{+/-}$ and *Tbx3*$^{+/+}$ littermates at E9.5 (Figure 2A-D, Table S1). In normal hearts, convergence positions the atria immediately posterior to the OFT (Figure 2A, B). In contrast, in *Tbx3*$^{-/-}$ embryos anterior displacement of the atria is delayed or defective, resulting in a gap between the OFT and atria (observed in 18/25 embryos; Figure 2C, D). This was accompanied in several cases by hypoplasia of the right ventricle and OFT of variable severity (Figure 2D, 5C). 4/25 *Tbx3*$^{-/-}$ embryos displayed a more severe phenotype in which a distended thin-walled heart tube looped ventrally and rightward looping and convergence were blocked (Figure 2E, F). In addition to a defect in looping we noted an overall developmental delay at this stage: the average somite number was 20.4±3.5 (n=32)

for *Tbx3*$^{+/+}$, 20.1±4.5 (n=48) for *Tbx3*$^{+/-}$, and 16.6±4.4 (n=29) for *Tbx3*$^{-/-}$ embryos ($p<0.001$, Student's t-test). Within litters, 27/29 (93%) of *Tbx3*$^{-/-}$ embryos were at or below the median somite number for the litter (n=14 litters).

Convergence occurs concomitantly with caudal displacement of the OFT in the pharyngeal region as bilateral arch arteries form sequentially in an anterior to posterior progression [20]. The tubular heart is initially connected to the 1st arch arteries, subsequently to the 1st and 2nd and then to the 3rd, 4th and 6th arch arteries, during which process the connection with the 1st and 2nd arch arteries is lost. We scored arch artery connections in *Tbx3*$^{-/-}$ embryos at E10.5 using a *Connexin40-eGFP* allele expressed in arterial endothelial cells [18]. A delay in caudal displacement of the OFT was observed such that whereas in *Tbx3*$^{+/-}$ and *Tbx3*$^{+/+}$ embryos the OFT was connected to the 3rd and 4th arch arteries and the connection with the 2nd arch artery no longer existed (Figure 2G, H), the OFT of somite-matched mutant embryos maintained a connection with the 2nd arch artery (Figure 2I, J). This phenotype was observed in 9/10 mutant embryos (Figure 2K). Subsequently, posterior arch arteries are present in *Tbx3*$^{-/-}$ embryos at E11.5 and E12.5 (Figure 1; data not shown).

Molecular patterning of *Tbx3*$^{-/-}$ hearts

The above phenotypic analysis suggests that OFT defects in *Tbx3*$^{-/-}$ embryos arise as a result of incomplete looping and a delay in caudal displacement of the OFT. The anterior limit of two genes expressed at defined levels along the embryonic AP axis, *Hoxb1* and *Raldh2*, was unaltered in *Tbx3*$^{-/-}$ embryos suggesting that overall anterior-posterior patterning of the pharyngeal region is not perturbed (Figure S1A-D). *Nkx2-5* and *Tbx5* are expressed normally in *Tbx3*$^{-/-}$ hearts at E9.5 (Figure S1E-L) suggesting that *Tbx3* is not required for global cardiac patterning.

Tbx2 is closely related to *Tbx3* and is required to repress the expression of the chamber-specific genes *Csl, Cx40,* and *Nppa* in AVC myocardium at E9.5[9,13,14]. As *Tbx3* is also expressed in AVC myocardium [8,12], patterning of the prospective chambers and AVC was analyzed in *Tbx3*$^{-/-}$ mutant embryos. Expression of *Tbx2* in the OFT and AVC is unaffected in *Tbx3*$^{-/-}$ hearts (Figure 3A-D). Similarly, *Tbx3* expression is normal in *Tbx2*$^{-/-}$ hearts at E9.5 suggesting that the AVC expression domains of *Tbx2* and *Tbx3* are not inter-dependent [9]. Expression of *Csl, Nppa* and *Cx40* is not expanded in the AVC of *Tbx3*$^{-/-}$ embryos (Figure 3E-J), revealing that AVC specification proceeds normally in the absence of *Tbx3*. Precocious expression of *Nppa* was observed in atrial myocardium of somite matched *Tbx3*$^{-/-}$ embryos at E9.5 (Fig 3G, H); however, no differences were observed at E10 (data not shown). As *Tbx2* and *Tbx3* interact genetically during mammary gland development [21], we explored a potential interaction of *Tbx2* and *Tbx3* during cardiac development. *Nppa*, *Csl* and *Cx40* transcripts did not accumulate in AVC myocardium of *Tbx2*$^{+/-}$; *Tbx3*$^{+/-}$ double heterozygous mutant embryos at E9.5 (Fig 3K, L; data not shown).

Tbx3 controls outflow tract elongation

In addition to AVC myocardium, *Tbx3* transcripts are observed in the pharyngeal region at E9.5 (Figure 4A, B) [8,12]. Analysis of Tbx3 protein distribution revealed that the caudal pharyngeal region expression domain includes ectoderm, pericardium, ventral pharyngeal endoderm and mesenchymal cells (Figure 4C-F). Tbx3 distribution was compared to that of nuclear localized β-galactosidase in embryos carrying the *Mlc1v-nlacZ-24* transgene, expressed in pharyngeal mesoderm and OFT myocardium as a result of integration upstream of the gene encoding Fibroblast growth factor 10[19]. Within the heart, Tbx3 positive nuclei are observed in AVC myocardium whereas β-galactosidase positive nuclei are found in myocardium of the right ventricle and OFT. A reciprocal distribution of Tbx3 and β-galactosidase positive nuclei was observed in pharyngeal mesenchyme (Figure 4D-F), such

that most cells expressed one or other epitope but not both. These results suggest that *Tbx3* is expressed in NC cells adjacent to the SHF. Immunohistochemistry with AP-2α revealed that Tbx3 and Ap-2α positive nuclei colocalize in mesenchymal cells in the caudal pharynx, confirming that these cells are NC-derived (Figure 4G-I). The contribution of NC cells to the OFT was investigated in *Tbx3*$^{-/-}$ mutant hearts. *Crabp1* expressing and Ap-2α positive NC cells were observed in the pharyngeal region of *Tbx3*$^{-/-}$ embryos (Figure S2A-D). Subsequently, *PlexinA2* expressing cells were observed in the distal OFT cushions of *Tbx3*$^{-/-}$ embryos in a pattern similar to that in control hearts, revealing that NC cells colonize the *Tbx3*$^{-/-}$ OFT (Figure S2E-H).

The OFT defects observed in *Tbx3*$^{-/-}$ embryos suggest that *Tbx3* might act indirectly on SHF deployment. Expression of the *Mlc1v-nlacZ-24* transgene in SHF cells in the dorsal pericardial wall was observed in *Tbx3*$^{+/-}$ and *Tbx3*$^{-/-}$ embryos (Fig 5B, D), even in embryos with severe OFT and right ventricular hypoplasia (Fig 5C, D). *Isl1* transcripts accumulate normally in the SHF of *Tbx3*$^{-/-}$ embryos (Fig 5E, F) and Isl1 protein was observed in pharyngeal mesoderm and the distal OFT of *Tbx3*$^{-/-}$ embryos; however, less Isl1 positive cells were observed in the OFT of hypoplastic hearts (Fig 5G, H). Quantitative analysis at E10.5 demonstrated a significant reduction in OFT length in *Tbx3*$^{-/-}$ compared to *Tbx3*$^{+/+}$ ($p<0.05$) and *Tbx3*$^{+/-}$ ($p<0.01$) embryos; in contrast, the mutant OFT was significantly broader than that of control littermates (Figure S3). These data reveal a failure of normal OFT elongation and morphogenesis in the absence of *Tbx3*.

Signaling molecules required for OFT elongation were evaluated in *Tbx3*$^{-/-}$ embryos. *Fgf8* transcripts are normally detectable in the SHF and OFT and were slightly elevated in the distal OFT of *Tbx3*$^{-/-}$ embryos (Figure 6A, B) [22,23]. *Bmp4* is expressed in the distal OFT and has been implicated in recruitment of SHF cells to the arterial pole of the heart [24]. A slight reduction in *Bmp4* transcript levels was observed in the OFT of *Tbx3*$^{-/-}$ embryos (Figure 6C, D). Quantitative RT-PCR revealed a significant increase in *Fgf8* (1.5-fold) and *Fgf10* (2-fold) transcript levels in the distal OFT and ventral pharynx of *Tbx3*$^{-/-}$ embryos; in contrast, *Bmp4* transcript levels were reduced (0.6-fold; Figure S4). Downstream mediators of FGF signaling were evaluated. *Pea3* transcript levels were slightly elevated in the caudal pharynx and an increase in phospho-ERK was observed in SHF cells in ventral pharyngeal mesoderm of *Tbx3*$^{-/-}$ embryos, consistent with elevated FGF signaling (Figure 6E-H). Shh in ventral pharyngeal endoderm regulates addition of SHF cells to the heart tube[25]; a reduction in *Shh* expression dorsal to the heart was observed in *Tbx3*$^{-/-}$ embryos (Figure S5A, B). Pitx2 is required in the SHF for normal OFT development [26]. While *Pitx2* transcripts are maintained in the first arch and in pharyngeal mesoderm, expression in the OFT was reduced in *Tbx3*$^{-/-}$ embryos (Fig S5C, D). Expression of *Wnt11,* which functions downstream of *Pitx2* in OFT development [27], was slightly reduced in *Tbx3*$^{-/-}$ embryos (Figure S5E, F)*; TGFβ2*, downstream of *Wnt11*[27], was also reduced in the OFT and pharyngeal region of *Tbx3*$^{-/-}$ embryos (Figure S5G, H) [17]. Loss of *Tbx3* is thus associated with altered gene expression affecting multiple signaling pathways implicated in SHF and OFT development.

To further analyze SHF development in *Tbx3*$^{-/-}$ embryos we evaluated differentiation, cell death and proliferation within pharyngeal mesoderm at E9.5. We found no evidence of precocious or delayed myocardial differentiation. Normal accumulation of sarcomeric myosin heavy chain was observed in the distal OFT of *Tbx3*$^{-/-}$ embryos and not in adjacent splanchnic mesodermal cells (Fig 7A-C). No significant differences in cell survival between *Tbx3*$^{+/-}$ and *Tbx3*$^{-/-}$ embryos were observed in pharyngeal mesoderm using Caspase3 immunohistochemistry (data not shown). However, a significant increase in proliferation of pharyngeal mesoderm was observed in *Tbx3*$^{-/-}$ embryos (Fig 7D-F). Using a BrdU incorporation assay in *Mlc1v-nlacZ-24* transgenic embryos, we observed a 20% increase in

the percentage of BrdU positive lacZ-positive SHF cells in *Tbx3*$^{-/-}$ versus *Tbx3*$^{+/-}$ embryos versus (Fig 7F, based on counts from 3 *Tbx3*$^{+/-}$ and 3 *Tbx3*$^{-/-}$ embryos; $p<0.001$, Student's t-test). In contrast, no difference was detected in BrdU incorporation in adjacent β-galactosidase negative nuclei (Fig 7F).

Discussion

The coordinated development of different cell types is critical for arterial pole morphogenesis. In particular, interactions between SHF and NC cells orchestrate OFT elongation and septation [5]. Our results demonstrate that *Tbx3* is required for normal arterial pole extension: in the absence of *Tbx3* the heart tube fails to elongate correctly, the convergence step of looping is perturbed and resulting alignment anomalies include DORV, transposition of the great arteries and double inlet left ventricle, common congenital heart defects in man. *Tbx3* is expressed in pharyngeal endoderm and NC cells closely associated with the SHF. Our data suggest that *Tbx3* controls OFT development indirectly, through regulation of intercellular signaling pathways coordinating proliferation and deployment of the SHF.

Tbx3 and the related gene *Tbx2* are coexpressed in AVC myocardium. *Tbx2* plays a role in repressing a chamber myocardial phenotype [9,14]. Here we show that *Tbx3*$^{-/-}$ and *Tbx2*$^{+/-}$; *Tbx3*$^{+/-}$ embryos have normal AVC patterning, suggesting that *Tbx2* plays the major role in this process. Zebrafish *Tbx2* and *Tbx3* homologues have recently been shown to redundantly control looping of the fish heart by regulating proliferation in the AVC [17]. The same study proposed that looping defects in *Tbx3*$^{Neo/Neo}$ mutant mouse embryos are caused by a failure to reduce proliferation in future AVC myocardium. Here we show that OFT alignment defects in *Tbx3*$^{-/-}$ hearts result from incomplete looping, though our results suggest an alternative etiology of the looping defect. We propose that failure to elongate the heart tube underlies the convergence and caudal OFT displacement defects in *Tbx3*$^{-/-}$ embryos, reflecting a role for *Tbx3* in the regulation of SHF deployment. Furthermore, we propose that this regulation is indirect and may be mediated by NC cells or pharyngeal endoderm. A subset of *Tbx3*$^{-/-}$ embryos exhibit general growth failure and have severely affected hearts where both rightward looping and convergence are blocked, suggesting the existence of an earlier, potentially distinct, role for *Tbx3* in heart tube formation. Arch artery anomalies are observed in a subset of *Tbx3*$^{-/-}$ embryos at E12.5, revealing a later role for *Tbx3* in asymmetric arch artery remodeling. The lack of survival of *Tbx3*$^{-/-}$ embryos to fetal stages precludes investigation of whether this phenotype is linked to the earlier developmental delay.

The addition of SHF cells to the arterial pole of the heart is coordinated by signals from adjacent cell-types, including pharyngeal endoderm and NC cells. The signals and upstream regulators mediating such effects, however, largely remain to be identified. *Tbx3* is expressed in pharyngeal endoderm and NC cells in the pharyngeal region rather than in the SHF itself. Impaired NC function in the absence of *Tbx3* could result in defective proliferation and deployment of the SHF. In the chick, NC in the pharyngeal region is required for normal SHF development in addition to OFT septation [3–5]. NC ablation results in myocardial hypoplasia and alignment defects associated with a reduced contribution of SHF cells to the elongating heart tube [3,5]. FGF signaling is elevated in the pharynx of NC ablated embryos, leading to hyperpoliferation and defective differentiation of the SHF [28]. Reduction in FGF signaling has been shown to partially rescue the effects of NC ablation on the SHF [29]. Precise levels of FGF signaling are critical for SHF deployment as pharmacological or genetic reduction of FGF signaling in the absence of NC ablation also leads to defective SHF development in chick and mouse [22,23,28–30].

Our results suggest that transcriptional targets of Tbx3 function in signaling pathways that regulate SHF deployment. In NC cells Tbx3 target genes may modulate FGF signaling in the pharyngeal region and thus regulate SHF exposure to FGF ligands, similar to the situation in NC ablated chick embryos. Elevated *Pea3* transcript and phospho-ERK levels in the caudal pharyngeal region of *Tbx3*$^{-/-}$ embryos provide evidence for enhanced FGF signaling, and are likely to contribute to the increased proliferation observed in pharyngeal mesoderm. Perturbation of the balance between proliferation and differentiation may underlie the defects in SHF deployment and OFT morphogenesis resulting in a shorter, broader OFT. Loss of *Tbx3* also affects other signaling pathways known to regulate OFT elongation: BMP signaling promotes SHF accretion at the arterial pole and *Bmp4* expression in the distal OFT of *Tbx3*$^{-/-}$ embryos is decreased. Indeed, elevated *Fgf8* and decreased *Bmp4* expression suggest that differentiation of the SHF may be impaired in mutant embryos. The *Pitx2*/*Wnt11*/*TGFβ2* axis, required for normal OFT development [27], is downregulated in the absence of *Tbx3*. Finally, altered *Shh* expression suggests that endodermal signaling is also impaired in mutant embryos. Loss of *Tbx3* thus alters the balance of signaling molecules in the caudal pharynx, revealing a pleiotropic role for *Tbx3* in the control of pharyngeal development and SHF deployment. Ongoing experiments aim to identify *Tbx3* target genes and dissect the downstream signaling pathways required for SHF and OFT development. In addition, tissue-specific inactivation of *Tbx3* will address the relative importance of *Tbx3* expression in NC versus pharyngeal epithelia for heart tube elongation and the possible role of epigenetic effects secondary to haemodynamic changes. Although not part of the classically defined Ulnar Mammary syndrome phenotype, congenital heart defects have been reported in Ulnar Mammary patients [31]; our results identify *TBX3* as a candidate gene for human congenital heart defects affecting the arterial pole of the heart.

Supplementary Material

Refer to Web version on PubMed Central for supplementary material.

Acknowledgments

We thank Elana Ernstoff for technical assistance and Lucile Miquerol for *Connexin40*^{eGFP} mice.

Sources of funding

This work was supported by the Inserm Avenir program, the Fondation de France, the Fondation pour la Recherche Medicale, the European Community's Sixth Framework Programme contract ('HeartRepair') LSHM-CT-2005-018630 (RGK) and a grant from the National Institutes of Health RO1 HD033082 (VEP).

References

1. Sugishita Y, Watanabe M, Fisher SA. The development of the embryonic outflow tract provides novel insights into cardiac differentiation and remodeling. Trends in Cardiovascular Medicine 2004;14:235–241. [PubMed: 15451515]
2. Buckingham M, Meilhac S, Zaffran S. Building the mammalian heart from two sources of myocardial cells. Nature Reviews 2005;6:826–835.
3. Yelbuz TM, Waldo KL, Zhang X, Zdanowicz M, Parker J, Creazzo TL, Johnson GA, Kirby ML. Myocardial volume and organization are changed by failure of addition of secondary heart field myocardium to the cardiac outflow tract. Developmental Dynamics 2003;228:152–160. [PubMed: 14517987]
4. Hutson MR, Kirby ML. Model systems for the study of heart development and disease. Cardiac neural crest and conotruncal malformations. Seminars in Cell & Developmental Biology 2007;18:101–110. [PubMed: 17224285]

5. Waldo KL, Hutson MR, Stadt HA, Zdanowicz M, Zdanowicz J, Kirby ML. Cardiac neural crest is necessary for normal addition of the myocardium to the arterial pole from the secondary heart field. Developmental Biology 2005;281:66–77. [PubMed: 15848389]
6. Naiche LA, Harrelson Z, Kelly RG, Papaioannou VE. T-box genes in vertebrate development. Annual Review of Genetics 2005;39:219–239.
7. Hoogaars WM, Barnett P, Moorman AF, Christoffels VM. T-box factors determine cardiac design. Cell Mol Life Sci 2007;64:646–660. [PubMed: 17380306]
8. Chapman DL, Garvey N, Hancock S, Alexiou M, Agulnik SI, Gibson-Brown JJ, Cebra-Thomas J, Bollag RJ, Silver LM, Papaioannou VE. Expression of the T-box family genes, Tbx1-Tbx5, during early mouse development. Developmental Dynamics 1996;206:379–390. [PubMed: 8853987]
9. Harrelson Z, Kelly RG, Goldin SN, Gibson-Brown JJ, Bollag RJ, Silver LM, Papaioannou VE. Tbx2 is essential for patterning the atrioventricular canal and for morphogenesis of the outflow tract during heart development. Development 2004;131:5041–5052. [PubMed: 15459098]
10. Davenport TG, Jerome-Majewska LA, Papaioannou VE. Mammary gland, limb and yolk sac defects in mice lacking Tbx3, the gene mutated in human ulnar mammary syndrome. Development 2003;130:2263–2273. [PubMed: 12668638]
11. Bamshad M, Lin RC, Law DJ, Watkins WC, Krakowiak PA, Moore ME, Franceschini P, Lala R, Holmes LB, Gebuhr TC, Bruneau BG, Schinzel A, Seidman JG, Seidman CE, Jorde LB. Mutations in human TBX3 alter limb, apocrine and genital development in ulnar-mammary syndrome. Nature Genetics 1997;16:311–315. [PubMed: 9207801]
12. Hoogaars WM, Tessari A, Moorman AF, de Boer PA, Hagoort J, Soufan AT, Campione M, Christoffels VM. The transcriptional repressor Tbx3 delineates the developing central conduction system of the heart. Cardiovascular Research 2004;62:489–499. [PubMed: 15158141]
13. Habets PE, Moorman AF, Clout DE, van Roon MA, Lingbeek M, van Lohuizen M, Campione M, Christoffels VM. Cooperative action of Tbx2 and Nkx2.5 inhibits ANF expression in the atrioventricular canal: implications for cardiac chamber formation. Genes & Development 2002;16:1234–1246. [PubMed: 12023302]
14. Christoffels VM, Hoogaars WM, Tessari A, Clout DE, Moorman AF, Campione M. T-box transcription factor Tbx2 represses differentiation and formation of the cardiac chambers. Developmental Dynamics 2004;229:763–770. [PubMed: 15042700]
15. Mommersteeg MT, Hoogaars WM, Prall OW, de Gier-de Vries C, Wiese C, Clout DE, Papaioannou VE, Brown NA, Harvey RP, Moorman AF, Christoffels VM. Molecular pathway for the localized formation of the sinoatrial node. Circulation Research 2007;100:354–362. [PubMed: 17234970]
16. Hoogaars WM, Engel A, Brons JF, Verkerk AO, de Lange FJ, Wong LY, Bakker ML, Clout DE, Wakker V, Barnett P, Ravesloot JH, Moorman AF, Verheijck EE, Christoffels VM. Tbx3 controls the sinoatrial node gene program and imposes pacemaker function on the atria. Genes & Development 2007;21:1098–1112. [PubMed: 17473172]
17. Ribeiro I, Kawakami Y, Buscher D, Raya A, Rodriguez-Leon J, Morita M, Rodriguez Esteban C, Izpisua Belmonte JC. Tbx2 and Tbx3 regulate the dynamics of cell proliferation during heart remodeling. PLoS ONE 2007;2:e398. [PubMed: 17460765]
18. Miquerol L, Meysen S, Mangoni M, Bois P, van Rijen HV, Abran P, Jongsma H, Nargeot J, Gros D. Architectural and functional asymmetry of the His-Purkinje system of the murine heart. Cardiovascular Research 2004;63:77–86. [PubMed: 15194464]
19. Kelly RG, Brown NA, Buckingham ME. The arterial pole of the mouse heart forms from Fgf10-expressing cells in pharyngeal mesoderm. Developmental Cell 2001;1:435–440. [PubMed: 11702954]
20. Kirby ML, Waldo KL. Neural crest and cardiovascular patterning. Circulation Research 1995;77:211–215. [PubMed: 7614707]
21. Jerome-Majewska LA, Jenkins GP, Ernstoff E, Zindy F, Sherr CJ, Papaioannou VE. Tbx3, the ulnar-mammary syndrome gene, and Tbx2 interact in mammary gland development through a p19Arf/p53-independent pathway. Developmental Dynamics 2005;234:922–933. [PubMed: 16222716]

22. Ilagan R, Abu-Issa R, Brown D, Yang YP, Jiao K, Schwartz RJ, Klingensmith J, Meyers EN. Fgf8 is required for anterior heart field development. Development 2006;133:2435–2445. [PubMed: 16720880]

23. Park EJ, Ogden LA, Talbot A, Evans S, Cai CL, Black BL, Frank DU, Moon AM. Required, tissue-specific roles for Fgf8 in outflow tract formation and remodeling. Development 2006;133:2419–2433. [PubMed: 16720879]

24. Waldo KL, Kumiski DH, Wallis KT, Stadt HA, Hutson MR, Platt DH, Kirby ML. Conotruncal myocardium arises from a secondary heart field. Development 2001;128:3179–3188. [PubMed: 11688566]

25. Goddeeris MM, Schwartz R, Klingensmith J, Meyers EN. Independent requirements for Hedgehog signaling by both the anterior heart field and neural crest cells for outflow tract development. Development 2007;134:1593–1604. [PubMed: 17344228]

26. Liu C, Liu W, Palie J, Lu MF, Brown NA, Martin JF. Pitx2c patterns anterior myocardium and aortic arch vessels and is required for local cell movement into atrioventricular cushions. Development 2002;129:5081–5091. [PubMed: 12397115]

27. Zhou W, Lin L, Majumdar A, Li X, Zhang X, Liu W, Etheridge L, Shi Y, Martin J, Van de Ven W, Kaartinen V, Wynshaw-Boris A, McMahon AP, Rosenfeld MG, Evans SM. Modulation of morphogenesis by noncanonical Wnt signaling requires ATF/CREB family-mediated transcriptional activation of TGFbeta2. Nature Genetics 2007;39:1225–1234. [PubMed: 17767158]

28. Farrell MJ, Burch JL, Wallis K, Rowley L, Kumiski D, Stadt H, Godt RE, Creazzo TL, Kirby ML. FGF-8 in the ventral pharynx alters development of myocardial calcium transients after neural crest ablation. The Journal of Clinical Investigation 2001;107:1509–1517. [PubMed: 11413158]

29. Hutson MR, Zhang P, Stadt HA, Sato AK, Li YX, Burch J, Creazzo TL, Kirby ML. Cardiac arterial pole alignment is sensitive to FGF8 signaling in the pharynx. Developmental Biology 2006;295:486–497. [PubMed: 16765936]

30. Vitelli F, Taddei I, Morishima M, Meyers EN, Lindsay EA, Baldini A. A genetic link between Tbx1 and fibroblast growth factor signaling. Development Oct;2002 129:4605–4611. [PubMed: 12223416]

31. Meneghini V, Odent S, Platonova N, Egeo A, Merlo GR. Novel TBX3 mutation data in families with Ulnar-Mammary syndrome indicate a genotype-phenotype relationship: mutations that do not disrupt the T-domain are associated with less severe limb defects. European Journal of Medical Genetics 2006;49:151–158. [PubMed: 16530712]

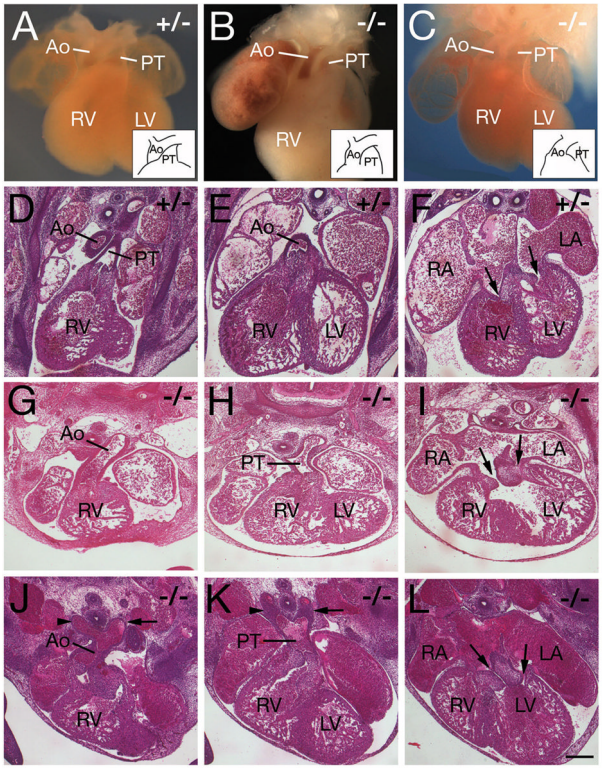

Figure 1.

Cardiac defects in *Tbx3* mutant embryos. A-C, wholemount views; D-L, paraffin sections counterstained with haemotoxylin and eosin. (A) *Tbx3*$^{+/-}$ E12.5 heart showing the pulmonary trunk (PT) positioned ventrally and the ascending aorta (Ao) dorsally. (B) *Tbx3*$^{-/-}$ E13.5 heart showing the Ao and PT aligned side by side above the right ventricle. (C) *Tbx3*$^{-/-}$ E12.5 heart with a ventrally positioned Ao and dorsally positioned PT (transposition-type DORV). Insets in A-C schematize the position of the Ao and PT. (D-F) *Tbx3*$^{+/-}$ E12.5 heart showing the PT aligned with the right ventricle (D), the ascending Ao with the left ventricle (E) and left and right atria with left and right ventricles, respectively (arrows in F). (G-I) *Tbx3*$^{-/-}$ E12.5 heart showing transposition-type DORV with a ventrally positioned Ao aligned with the right ventricle (G), dorsally positioned PT (H) and a connection between both atria and the left ventricle (arrows in I). (J-L) *Tbx3*$^{-/-}$ E12.5 heart with a ventrally positioned Ao aligned with the right ventricle (J), dorsally positioned PT (K) and DILV (arrows in L). Note the abnormal persistence of the right 4th (arrowhead in J) and right 6th (arrowhead in K) aortic arch arteries, in addition to left arch arteries (arrows in J, K). RV, right ventricle; LV, left ventricle; RA, right atrium; LA, left atrium. Scale bar (D-L): 200μm.

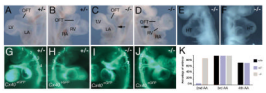

Figure 2.

Looping defects and delayed aortic arch artery formation in *Tbx3* mutant embryos. Left (A, C, E) and right (B, D, F) views of E9.5 $Tbx3^{+/-}$ (A, B) and $Tbx3^{-/-}$ (C-F) embryos. A convergence defect can be observed as a gap between the OFT and atria not present in normal embryos (arrows). Note the hypoplastic OFT and right ventricle (RV) in the $Tbx3^{-/-}$ embryo (D, compared to B). (E, F) Severely affected $Tbx3^{-/-}$ embryo showing an overall developmental delay. Note the thin walled dilated heart tube with a ventral loop. (G-K) $Cx40^{eGFP}$ expression shown in left (G, I) and right (H, J) views of $Tbx3^{+/-}$; $Cx40^{eGFP+/-}$ (G, H) and $Tbx3^{-/-}$; $Cx40^{eGFP+/-}$ (I, J) embryos at E10.5 (35 and 34 somites respectively). eGFP fluorescence in arterial endothelial cells shows that the aortic sac is connected to the 3rd and 4th arch arteries in the $Tbx3^{+/-}$ embryo (G, H). In contrast, the 2nd arch arteries are still connected to the aortic sac and the 4th arch artery is not yet apparent in the $Tbx3^{-/-}$ embryo (I, J). (K) Histogram showing the percentage of somite matched embryos in which the aortic sac is connected to the 2nd, 3rd and 4th aortic arch artery (AA) at E10.5. LA, left ventricle; LA left atrium; RA, right atrium.

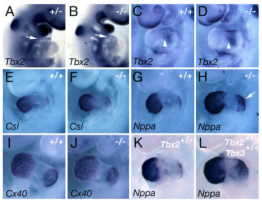

Figure 3.

Molecular patterning in *Tbx3*$^{-/-}$ embryos. Whole-mount views of E9.5 *Tbx3*$^{+/-}$(A), *Tbx3*$^{+/+}$ (C, E, G, I), *Tbx3*$^{-/-}$ (B, D, F, H, J), *Tbx2*$^{+/-}$ (K) and *Tbx2*$^{+/-}$; *Tbx3*$^{+/-}$ (L) embryos after in situ hybridization. *Tbx2* is expressed normally in the OFT (A, B, arrows) and AVC (C,D, arrowheads) of *Tbx3*$^{-/-}$ embryos. *Csl* (E, F), *Nppa* (G, H) and *Cx40* (I, J) are expressed in working atrial and ventricular myocardium and do not accumulate in the AVC of *Tbx3*$^{-/-}$ hearts. Note that *Nppa* is precociously upregulated in atrial myocardium of *Tbx3*$^{-/-}$ hearts (arrow). (K, L) *Tbx2*$^{+/-}$ and *Tbx2*$^{+/-}$; *Tbx3*$^{+/-}$ double heterozygous embryos do not accumulate *Nppa* transcripts in the AVC.

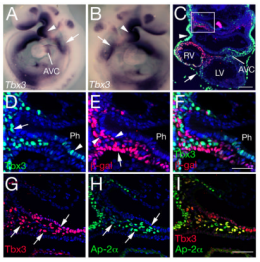

Figure 4.

Tbx3 expression in the pharyngeal region. (A, B) *Tbx3* in situ hybridization at E9.5. *Tbx3* is expressed in the first branchial arch (arrowhead), caudal pharynx (arrow) and atrioventricular canal (AVC). (C-F) Immunohistochemistry with anti-Tbx3 (green) and anti-β-galactosidase (red) antibodies in a transverse section through the caudal pharynx and heart of an E9.5 embryo carrying the *Mlc1v-nlacZ-24* transgene. Tbx3 protein is observed in the AVC, ectoderm (arrowhead), pericardium (arrow), pharyngeal endoderm and NC cells (box in C); β-galactosidase is observed in right ventricular myocardium and the dorsal pericardial wall. (D-F) High magnification of the boxed region in C showing the reciprocal distribution of Tbx3 and β-galactosidase in caudal pharyngeal mesenchyme. Tbx3 is observed in pharyngeal endoderm (arrowhead in D) and NC derived mesenchyme (arrow). β-galactosidase is observed in pharyngeal mesoderm (arrowheads in E) including the SHF (arrow). (G-I) Immunohistochemistry with anti-Tbx3 (red) and anti-AP-2α (green) antibodies. Ap-2α colocalises with Tbx3 in pharyngeal ectoderm and NC derived mesenchyme (arrowheads). Ph, pharynx. Scale bars (C) 100μm; (D-I): 50μm.

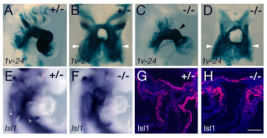

Figure 5.

Second heart field and outflow tract defects in *Tbx3* mutant embryos. (A-D) X-gal stained E9.5 *Mlc1v-nlacZ-24* transgenic embryos in right lateral (A, C) and ventral views with the heart removed (B, D). SHF cells in the dorsal pericardial wall are indicated by white arrowheads. Note the hypoplastic OFT and right ventricle in the embryo in panel C (arrowhead) and reduced transgene expression in the second arch. (E, F) *Isl1* transcripts accumulate normally in the pharyngeal region of $Tbx3^{-/-}$ embryos. (G, H) Isl1 protein is observed in pharyngeal mesoderm and OFT myocardium of $Tbx3^{+/-}$ and $Tbx3^{-/-}$ hearts. Scale bar: 100μm.

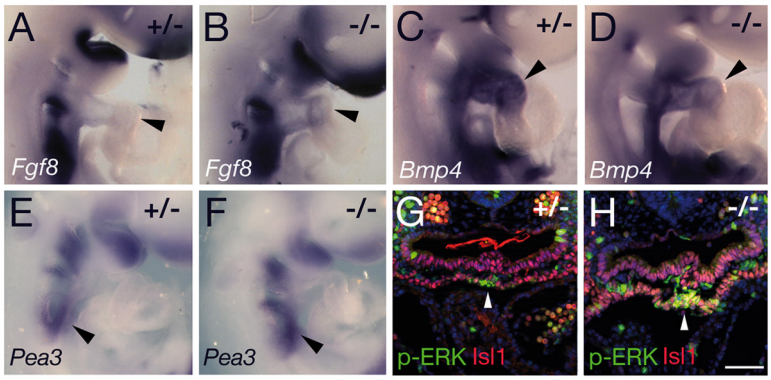

Figure 6.

Analysis of signaling pathways in *Tbx3* mutant embryos at E9.5. (A, B) In situ hybridization showing elevated levels of *Fgf8* transcript accumulation in the OFT of $Tbx3^{-/-}$ (B) relative to $Tbx3^{+/-}$ (A) embryos (arrowheads). (C, D) *Bmp4* transcripts are reduced in the OFT of $Tbx3^{-/-}$ (D) relative to $Tbx3^{+/-}$ (C) hearts (arrowheads). (E, F) *Pea3* transcripts are slightly upregulated in the caudal pharynx of $Tbx3^{-/-}$ embryos (F, arrowhead). (G, H) Fluorescent immunohistochemistry showing elevated levels of nuclear phospho-ERK (green) in Isl1-positive ventral pharyngeal mesoderm (red) of $Tbx3^{-/-}$ (H, arrowhead) compared to $Tbx3^{+/-}$ embryos (G). Scale bar (G, H): 100μm.

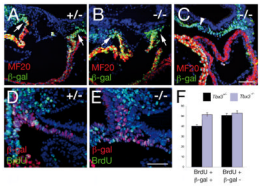

Figure 7.

Properties of the second heart field in *Tbx3* mutant embryos. (A-C) Immunohistochemistry with MF20 anti-sarcomeric myosin and anti-β-galactosidase antibodies in paraffin sections of E9.5 $Tbx3^{+/-}$ (A) and $Tbx3^{-/-}$ (B, C) embryos carrying the *Mlc1v-nlacZ-24* transgene. (A-C) No differentiated cardiomyocytes are observed in mesoderm adjacent to the OFT (arrows) or in the dorsal pericardial wall (arrowheads) of $Tbx3^{+/-}$ or $Tbx3^{-/-}$ embryos. Immunohistochemistry with anti-BrdU and anti-β-galactosidase antibodies in paraffin sections of E9.5 $Tbx3^{+/-}$ (D) and $Tbx3^{-/-}$ (E) embryos carrying the *Mlc1v-nlacZ-24* transgene and treated with BrdU in utero. (F) Histogram showing the percentage of β-galactosidase positive and negative nuclei that are BrdU positive. There is a 20% increase in BrdU positive β-galactosidase positive nuclei in $Tbx3^{-/-}$ compared to $Tbx3^{+/-}$ embryos ($p<0.001$, Student's t-test). Nuclei are labeled with Hoechst (blue). Scale bar (A-C): 100μm; (D, E): 50μm.

Table 1

Incidence of heart defects in *Tbx3*$^{-/-}$ embryos at E12.5 and E13.5

Defect	*Tbx3*$^{-/-a}$
Double outlet right ventricle	5/12
Double outlet right ventricle with transposition	7/12
Double inlet left ventricle	9/12
Persistent right 4th pharyngeal arch artery	9/12
Persistent right 6th pharyngeal arch artery	5/12

[a]Data from 6 E12.5 and 6 E13.5 *Tbx3*$^{-/-}$ embryos; no abnormalities were observed in *Tbx3*$^{+/+}$ and *Tbx3*$^{+/-}$ littermates.